



Technical note: in-situ measurements and modelling of the oxidation kinetics in films of a cooking aerosol proxy using a Quartz Crystal Microbalance with Dissipation monitoring (QCM-D)

5 Adam Milsom¹, Shaojun Qi², Ashmi Mishra³, Thomas Berkemeier³, Zhenyu Zhang² and Christian Pfrang^{1,4}

¹School of Geography, Earth and Environmental Sciences, University of Birmingham, Edgbaston, B15 2TT, Birmingham, UK.

10 ²School of Chemical Engineering, University of Birmingham, Edgbaston, B15 2TT, Birmingham, UK.

³Multiphase Chemistry Department, Max Planck Institute for Chemistry, Hahn-Meitner-Weg 1, 55128 Mainz, Germany.

⁴Department of Meteorology, University of Reading, Whiteknights, Earley Gate, RG6 6BB, Reading, UK.

Correspondence to: Christian Pfrang (c.pfrang@bham.ac.uk)

Abstract. Aerosols and films are found in indoor and outdoor environments. How they interact with pollutants, such as ozone, has a direct impact on our environment via cloud droplet formation and the chemical persistence of toxic aerosol constituents. The chemical reactivity of aerosol emissions is typically measured spectroscopically or by techniques such as mass spectrometry, directly monitoring the amount of material during a chemical reaction. We present a study which indirectly measures oxidation kinetics in a common cooking aerosol proxy using a low-cost Quartz Crystal Microbalance with Dissipation monitoring (QCM-D). We validated this approach by comparison with kinetics measured both spectroscopically and with high-intensity synchrotron radiation. Using microscopy, we found that the film morphology changed and film rigidity increased during oxidation. There was evidence of surface crust formation on oxidised particles, though this was not consistent for all experiments. Crucially, our kinetic modelling of these experimental data confirmed that the oleic acid decay rate is in line with previous literature determinations, which demonstrates that performing such experiments on a QCM-D does not alter the underlying mechanism. There is clear potential to take this robust and low cost, but sensitive method to the field for in-situ monitoring of reactions outdoors and indoors.

1 Introduction

Air quality is impacted by both natural and anthropogenic factors such as meteorology and cooking emissions (Chan and Yao, 2008; Huang et al., 2021), with cooking emissions estimated to contribute up to 10% of PM_{2.5} in the UK (Ots et al., 2016). In



the West, people spend ~90% of their time indoors (Klepeis et al., 2001), and indoor air quality research has become important
30 in recent years. Recent field studies have demonstrated the marked effect of processes such as cooking, cleaning and occupancy
on indoor air quality in terms of particulate matter and volatile organic compound (VOC) emissions (Liu et al., 2021; Patel et
al., 2020).

Surface films are present in the indoor environment and are formed by the deposition of particles and condensation
of semi-volatile species with typical thicknesses in the order of a few hundred nanometres (Ault et al., 2020; Or et al., 2018).
35 Indoor surface film chemistry is particularly important for air quality due to the high surface-to-volume ratio compared with
outdoors. The composition of indoor films can vary between rooms and is influenced by the emission sources in each room
(Or et al., 2018). For example, film samples collected in a kitchen after a stir-fry episode are likely to contain a larger amount
of organic material including fatty acids (Or et al., 2020), which are major constituents of common cooking oils (Wang et al.,
2020; Zahardis et al., 2006b).

40 Oleic acid is a major fatty acid component of cooking (Wang et al., 2020) and marine (Kirpes et al., 2019; Osterroht,
1993) organic emissions. As a surfactant, it can influence the cloud formation potential of aerosol particles, affecting the
climate indirectly (Ovadnevaite et al., 2017). Oleic acid is also used as a marker for urban cooking emissions and the ratio of
oleic acid to its saturated analogue (stearic acid) is a measure of how aged a sample of urban aerosols is (Wang et al., 2020).
For these reasons, oleic acid is a common model system used to study heterogeneous reactions with oxidants such as ozone
45 and NO₃ in the laboratory and with kinetic models (Berkemeier et al., 2021; Gallimore et al., 2017; King et al., 2004, 2009,
2020; Sebastiani et al., 2022; Shiraiwa et al., 2010, 2012; Woden et al., 2020; Zahardis and Petrucci, 2007). The atmospheric
lifetime of oleic acid is longer than has been predicted in laboratory experiments (Robinson et al., 2006; Rudich, 2003), with
recent evidence suggesting that the steric conformation of the fatty acid can impact on its chemical lifetime (Wang and Yu,
2021).

50 The viscosity of organic films and aerosols is an important factor in determining the rate at which heterogeneous
processing occurs (i.e. the rates of water and reactive gas uptake) (Davies and Wilson, 2016; Koop et al., 2011; Shiraiwa et
al., 2011). The ozonolysis of oleic acid is known to increase the viscosity (Hosny et al., 2016) and density (Katrib et al., 2005)
of the organic phase. An increase in viscosity decreases the rate of oxidative processing. Previous work has demonstrated that
a viscous self-organised form of oleic acid (Milsom et al., 2021a, 2022a; Pfrang et al., 2017) reacts approximately an order of
55 magnitude slower than the liquid form (Milsom et al., 2021b) and kinetic modelling of these results has shown that this could
lengthen the chemical lifetime of oleic acid by an order of days under typical atmospheric conditions (Milsom et al., 2022c).
There is a need for a technique that can measure both reaction kinetics and changes related to physical characteristics (i.e.
viscosity) simultaneously with a high time resolution.

In this study, we used a quartz crystal microbalance with dissipation monitoring (QCM-D) to follow the reaction of
60 oleic acid with ozone, which was complemented by white light interferometry (WLI) and Raman spectroscopy. Dissipation
monitoring allowed us to infer changes in film rigidity and microscopic techniques revealed morphological changes during
oxidation, including evidence for surface crust formation previously postulated and evidenced for this system (Milsom et al.,



2021b, 2022c). We derived kinetic decay constants from the QCM-D data and fitted a kinetic model to the Raman data to demonstrate the useful information that could be extracted from these experiments and to highlight the challenges associated with this technique. We then drew atmospheric implications from our findings and suggest future directions for this experiment.

2 Methodology

Oleic acid (Part ref. 364525, technical grade 90%, Sigma Aldrich), methanol (ACS reagent, 99.8%) and oxygen gas (BOC, 99.5%) were used without further purification. Silicon dioxide coated QCM sensors (5 MHz, 14 mm diameter, Cr/Au/SiO₂ surface, Quartz Pro, Sweden) were rinsed with ethanol followed by a cleaning process in an oxygen plasma chamber (HPT-100, Henniker Plasma) at an oxygen flow rate of 10 sccm for 5 min prior to the deposition of oleic acid.

An oleic acid solution (10wt.% in methanol) was freshly prepared. The cleaned QCM sensor was placed on a spin coater (SPIN150i, APT GmbH) and spun at 6000 rpm as 60 μ L oleic acid solution was added onto the sensor surface dropwise using a micro pipettor. Oleic acid coated sensors were tested the same day to avoid degradation due to the trace amount of ozone in the ambient atmosphere.

QCM-D works on the principle that the resonant frequency (f) of a piezoelectric quartz crystal can be monitored electronically. This f decreases when small amounts of material are added to the quartz crystal. The dissipation factor (D) is a measure of the energy dissipated by the deposited material (Voinova et al., 1999). Both f and D are functions of the deposited film viscoelasticity. Generally, a lower D implies a more rigid film.

The ozonolysis of oleic acid was studied using the coated sensors and a QCM-D (NEXT, openQCM, Italy), with which the frequency and energy dissipation history during the ozonolysis process was simultaneously recorded.

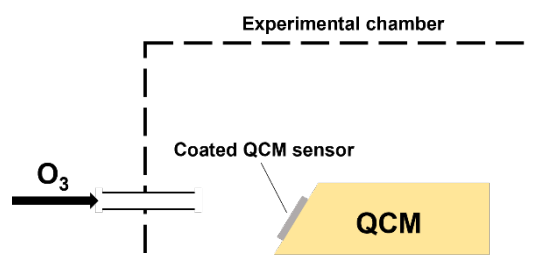


Figure 1. A schematic illustration of the experiment presented in this study.

An experimental chamber made of polystyrene and with the inner walls lined with aluminium foil was used for ozonolysis experiments (Fig. 1). Ozone was produced by flowing oxygen at 1.2 L min⁻¹ through a commercial pen-ray ozoniser (Ultraviolet Products Ltd, Cambridge, UK) which exposed the oxygen flow to UV radiation. The concentration of ozone was calibrated by UV-Visible spectroscopy and was determined to be 3.8 \pm 0.5 ppm.



90 A white light interferometer (WLI, resolution 20×; MicroXAM2, KLA Tencor, California, U.S.A) was employed to
establish the morphology of the oleic acid coated sensor. Scans were taken on each tested sensor at representative positions,
i.e. within the test window (dia. 7 mm) that was previously subject to ozonolysis, at boundary of the test window, and sites far
away from the test window. WLI data was analysed using an image processing program Gwyddion with which surface
parameters, including surface roughness, 2-D/3-D height profiles could also be extracted. Raman features of the as-prepared
and the ozone-exposed oleic acid coatings were captured with a confocal Raman spectrometer (inVia™ by Renishaw, 20x
optical magnification, laser wavelength 532 nm, laser power 10%). At least 30 accumulations were made to maximise the
95 signal-to-noise ratio.

Kinetic multi-layer models based on the Pöschl-Rudich-Ammann framework (Pöschl et al., 2007) are commonly used
to analyse oleic acid ozonolysis experiments (Berkemeier et al., 2021; Milsom et al., 2022c, 2022b; Shiraiwa et al., 2010,
2012). The kinetic multilayer model of aerosol surface and bulk chemistry (KM-SUB) was employed to describe the reaction
occurring between the deposited oleic acid and ozone (Shiraiwa et al., 2010). KM-SUB resolves processes such as gas
adsorption and desorption, bulk diffusion, as well as surface and bulk chemistry. Although the deposited films were collections
of smaller droplets, oleic acid was modelled as a flat film as the geometry was closer to that of a film for each individual
droplet due to the high spreading ratio of oleic acid on the quartz surface. A KM-SUB model developed specifically for oleic
acid decay data measured by Raman spectroscopy, and optimised to 12 literature datasets, was fitted to the Raman data
collected here (Berkemeier et al., 2021). A full description of the model is in the sect. S1 in the Supporting Information.

105

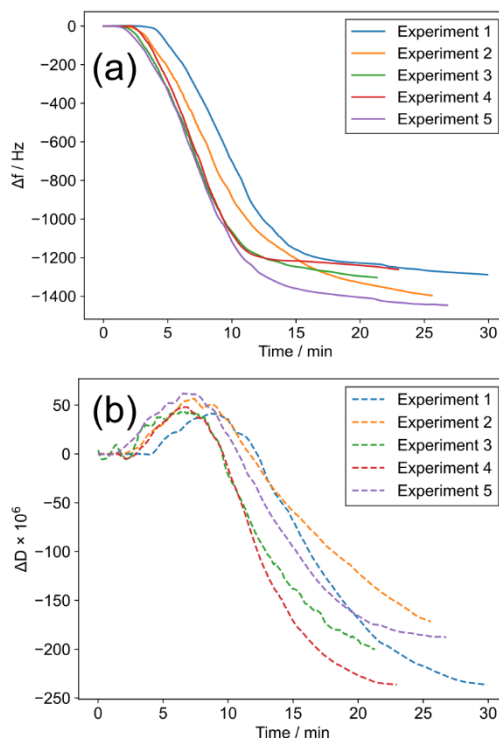
110

115



3 Results and Discussion

3.1 Kinetics of oleic acid ozonolysis



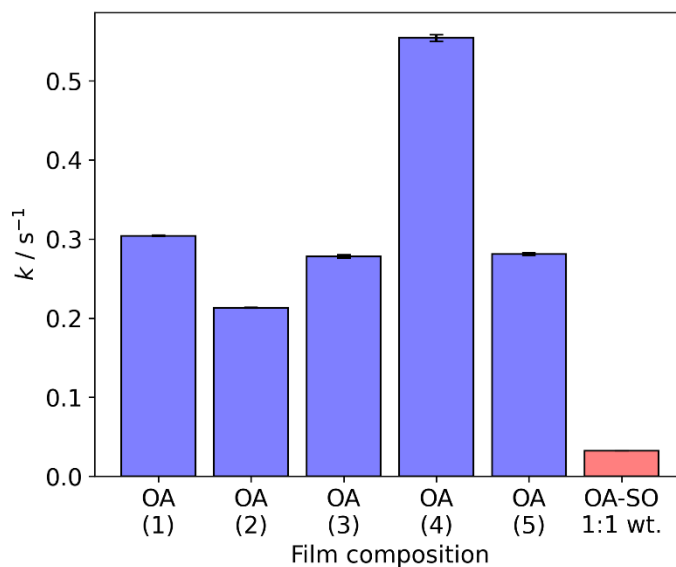
120 **Figure 2. (a) Δf vs time since the start of ozone exposure for five coatings. (b) ΔD vs time since the start of ozone exposure for five coatings, measured simultaneously to (a). The line colours link the same experiments in (a) and (b).**

We observed reproducible trends in f and D during ozone exposure (Fig. 2). After an initial build-up of ozone in the chamber, the resonant frequency shift (Δf) becomes more negative followed by a levelling off by the end of the experiment. This observation suggests an increase in mass per unit area on the QCM crystal surface via the Sauerbrey equation, which states that the mass per unit area deposited on a QCM crystal is inversely proportional to the crystal's measured resonant frequency
125 (Demou et al., 2003).

The apparent increase in mass per unit area observed during ozonolysis could be due to an increase in film density. This has been observed previously for oleic acid ozonolysis, where density increases from 0.89 to 1.12 g cm⁻³ with increasing ozone exposure, presumably due to ozonolysis products having higher densities (Katrib et al., 2005). This is also evidenced by the overall lower dissipation (negative ΔD) measured simultaneously with the QCM-D (Fig. 2(b)). More rigid coatings
130 dissipate less energy. Only nonanal and nonanoic acid are known to be volatile (Müller et al., 2022; Zahardis and Petrucci, 2007). The other products are assumed to remain in the condensed phase. Some products are oligomeric with higher molecular weights (Reynolds et al., 2006; Zahardis et al., 2006a). These are assumed to be more viscous and rigid than liquid oleic acid.



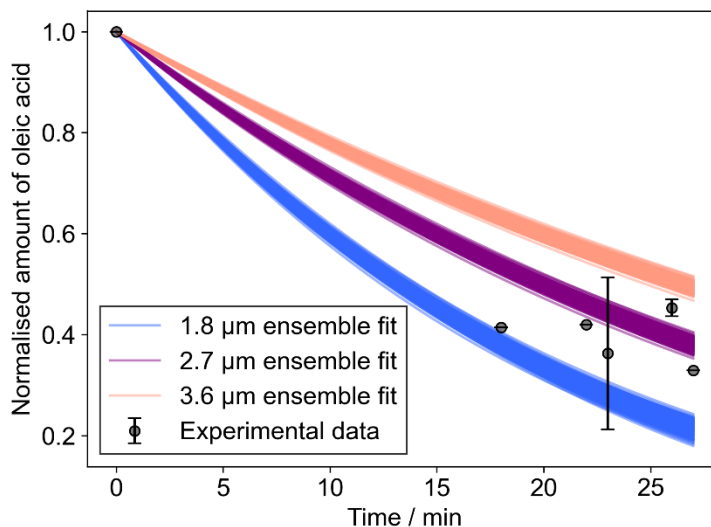
The formation of heavier molecules in the film along with film densification could explain the apparent increase in mass per unit area on the QCM crystal surface.



135 **Figure 3.** The pseudo-first order decay constant (k) measured at the fastest point of each Δf vs time plot presented in Fig. 2(a). The experiment numbers in brackets correspond with those presented in Fig. 2. The final bar is from the decay of a self-organised oleic acid-sodium oleate mixture analogous to previous work (Milsom et al., 2021b). All k values are measured at an ozone concentration of 3.8 ± 0.5 ppm. OA: oleic acid; OA-SO: oleic acid-sodium oleate mixture.

140 The pseudo-first order decay constants (k) are generally consistent and variation is most likely due to slight variations in initial film thickness (Fig. 3). Taking the point at which the decay in Δf is fastest returns a measure of the reaction kinetics. Although Δf is not a measure of the amount of reactant remaining on the surface, applying pseudo-first order reaction kinetic analysis to the region of fastest Δf decay can be used for comparisons with the same system (e.g. oleic acid) under different conditions. To test this, we coated a film of an oleic acid-sodium oleate (1:1 wt.) mixture and exposed it to the same oxidative conditions as the pure oleic acid films. This mixture is known to self-organise into lamellar bilayers and is semi-solid (Milsom et al., 2021b). We found that k for this viscous mixture was ~ 1 order of magnitude smaller than for the liquid oleic acid films presented here. This is consistent with the difference in reaction rates we have previously measured using X-ray scattering and Raman spectroscopy (Milsom et al., 2021b), validating this approach.

150



155 **Figure 4. The decay of oleic acid followed experimentally using the area of C=C Raman band at $\sim 1650\text{ cm}^{-1}$ normalised to the CH_2 band at $\sim 1452\text{ cm}^{-1}$. Ensemble outputs from a pre-optimised model of oleic acid ozonolysis (Berkemeier et al., 2021) are presented for a range of initial film thicknesses in the range measured by WLI.**

A kinetic model that has been pre-optimised to 12 unique datasets (Berkemeier et al., 2021) was applied to the experimental data measured by Raman spectroscopy (Fig. 4). Outputs from different model outputs with varying film thicknesses are presented as an ensemble of 167 optimised input parameter sets. The model also considers the formation of an oleic acid-Criegee intermediate adduct that would contribute to the carbon-carbon double bond signal observed in the Raman spectrum.

160 We found that the pre-optimised model fitted reasonably well to the experimental data when initialised at a thickness range determined by the range observed using WLI on films before ozone exposure (Fig. 4). The model does not describe changes in film morphology such as the coagulation of droplets into larger droplets, which was observed in the experiment (Fig. 5). Changes in the size of the deposited droplets will affect the uptake of ozone to oleic acid via changes to the surface area-to-volume ratio and the mixing time for ozone in the condensed phase (Pöschl et al., 2007). Therefore, A gradual increase of layer thickness will lead to a slowing of oleic acid consumption. We tested this hypothesis by splitting the model into 5 distinct time periods, each new period resulting in film thickening (Fig. S1 in the Supporting information). However, time-resolved morphological information would be required to constrain this particular feature. There could also be an effect from surface crust formation, slowing the reaction (Milsom et al., 2021a, 2022c; Pfrang et al., 2011). Though the exact kinetic effect of crust formation and morphology change cannot be deconvoluted here, we believe that the significant change in morphology (i.e. increase in average film size) dominates.

3.2 Morphology changes

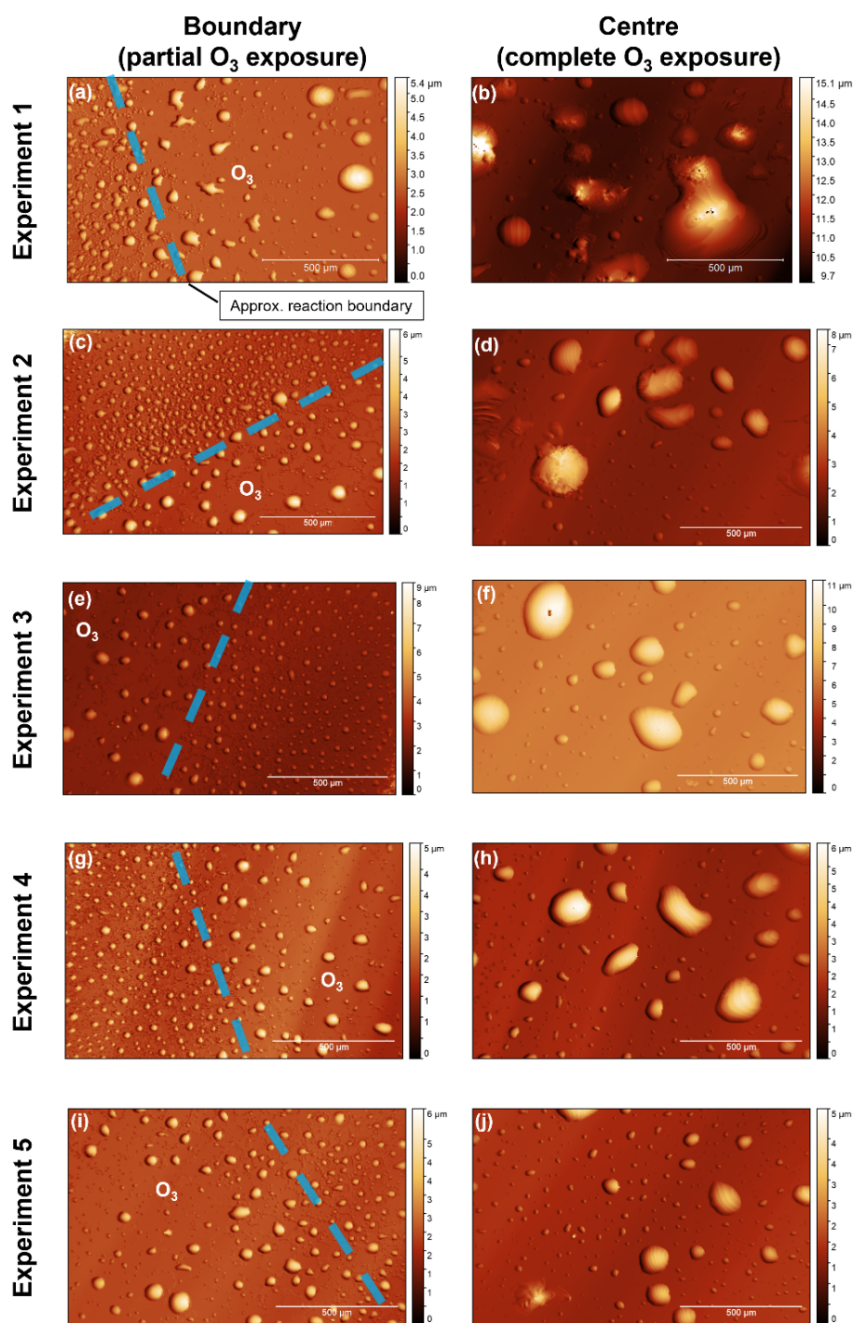


Figure 5. White light interferometry images of oleic acid coated QCM crystal surfaces for five separate ozonolysis experiments. Images were taken at the reaction boundary i.e. the outer region where the surface was not exposed to the oxygen-ozone mixture due to the design of the QCM crystal holder (the diameters of the crystal and the test window are 14 and 7 mm, respectively). The approximate location of the reaction boundary is illustrated. Images at the centre of the QCM crystal surface show particles fully exposed to the oxygen-ozone mixture. The approximate height of each droplet is indicated by the heatmap.



185 There is a difference in morphology between unoxidised and oxidised particles, with oxidation appearing to cause droplet coagulation (Fig. 5). The design of the QCM instrument, where the sample holder window had a smaller diameter than the QCM crystal, meant that only the central part of the QCM surface was exposed to ozone, with the outer regions of the surface not exposed to the chamber environment. This allowed us to image the boundary between these two regions and compare oxidised and unoxidised droplets. Initial droplet heights were mostly in the region of $\sim 1 - 9 \mu\text{m}$ with a mean height calculated as $\sim 2 \mu\text{m}$. After oxidation, coagulation occurred resulting in fewer, larger droplets with maximum heights of $\sim 10 - 15 \mu\text{m}$ (see sect. S3 for the representative height scans used for this analysis).

190 In addition to droplet coagulation, we observed microscopic evidence of a crust forming, triggered by film oxidation (Fig. 5). This was not consistent for all droplets, however some oxidised particles have clear rough patches on their surfaces as compared to the relatively smooth surfaces of other particles (Fig. 5(b) & (d)). There has been previous experimental and modelling evidence that crusts could form on the surface of oxidising oleic acid films and particles (Milsom et al., 2021a, 2021b, 2022c). Similar morphological changes have been observed by optical microscopy and atomic force microscopy (Hung and Tang, 2010; Liu et al., 2020). Here, WLI has confirmed the reproducible nature of these morphology changes along with
195 a more quantitative description of the particle size changes observed.

3.3 Atmospheric implications

We have demonstrated that the phase state of deposited oleic acid changes during ozonolysis. An increase in viscosity has been monitored before for the oleic acid-ozone system (Hosny et al., 2016). However, this involved adding a fluorescent probe molecule to the sample. Here, we confirm with the non-invasive QCM-D experiment that the deposited cooking aerosol proxy
200 becomes more rigid during ozonolysis.

A viscous layer coating aerosol material is thought to contribute to the persistence of pollutants in the atmosphere (Mu et al., 2018; Shrivastava et al., 2017). In this study, we have qualitatively observed a crust forming on the outside of oxidised oleic acid particles. We have previously observed a surface layer of aggregates forming during the ozonolysis of oleic acid-sodium oleate particles using X-ray scattering, which we assumed were high molecular weight products (Milsom et al.,
205 2021a). Modelling of the oleic acid-sodium oleate system also suggests a crust could form (Milsom et al., 2022c). Our microscopic evidence presented here was not consistent for all experiments. However, it does add to the growing body of evidence for crust formation, potentially increasing persistence of atmospheric pollutants co-emitted with oleic acid.

Conclusions

The high temporal resolution of QCM method presented here has allowed us to establish a measure of the ozonolysis kinetics
210 of a commonly studied cooking aerosol proxy. We have confirmed that the relative decay rate of oleic acid compared to a viscous form of oleic acid, measured using the QCM method, agrees with that derived using X-ray scattering and Raman spectroscopy (Milsom et al., 2021b). An analysis using a kinetic model, pre-optimised to 12 oleic acid ozonolysis datasets,



demonstrates that the oleic acid decay rate measured with the QCM method are consistent with previous experiments on aerosol particles in the literature (Berkemeier et al., 2021).

215 We can now qualitatively follow the rigidity, or phase state, of these oxidising films over time using the dissipation measured by the QCM-D instrument. For films of uniform thickness, there is the possibility of applying models of viscoelasticity to QCM-D data to derive the viscosity of coated films (Voinova et al., 1999). Future work should focus on this as a potential real-time measure of the viscosity of environmental films.

220 The portable QCM-D experiment described here could be used in the field to follow the kinetics of the interaction of real environmental films with pollutants (e.g. ozone and NO₂). Similar experiments have been carried out using a QCM regarding the water uptake of deposited films in the context of air quality and atmospheric chemistry (Asad et al., 2004; Demou et al., 2003; Schwartz-Narbonne and Donaldson, 2019).

Competing interests

At least one of the (co-)authors is a member of the editorial board of Atmospheric Chemistry and Physics.

225 Acknowledgements

This work was supported by NERC grant number NE/T00732X/1 and a NERC Discipline Hopping Grant number 1002711. A. Mishra was supported by the Max Planck Graduate Center with the Johannes Gutenberg-Universität Mainz (MPGC).

References

- 230 Asad, A., Mmereki, B. T. and Donaldson, D. J.: Enhanced uptake of water by oxidatively processed oleic acid, *Atmos. Chem. Phys.*, 4(8), 2083–2089, doi:10.5194/acp-4-2083-2004, 2004.
- Ault, A. P., Grassian, V. H., Carslaw, N., Collins, D. B., Destailhats, H., Donaldson, D. J., Farmer, D. K., Jimenez, J. L., McNeill, V. F., Morrison, G. C., O'Brien, R. E., Shiraiwa, M., Vance, M. E., Wells, J. R. and Xiong, W.: Indoor Surface Chemistry: Developing a Molecular Picture of Reactions on Indoor Interfaces, *Chem*, 6(12), 3203–3218, doi:10.1016/j.chempr.2020.08.023, 2020.
- 235 Berkemeier, T., Mishra, A., Mattei, C., Huisman, A. J., Krieger, U. K. and Pöschl, U.: Ozonolysis of Oleic Acid Aerosol Revisited: Multiphase Chemical Kinetics and Reaction Mechanisms, *ACS Earth Sp. Chem.*, 5(12), 3313–3323, doi:10.1021/acsearthspacechem.1c00232, 2021.
- Chan, C. K. and Yao, X.: Air pollution in mega cities in China, *Atmos. Environ.*, 42(1), 1–42, doi:10.1016/j.atmosenv.2007.09.003, 2008.
- 240 Davies, J. F. and Wilson, K. R.: Raman Spectroscopy of Isotopic Water Diffusion in Ultraviscous, Glassy, and Gel States in



- Aerosol by Use of Optical Tweezers, *Anal. Chem.*, 88(4), 2361–2366, doi:10.1021/acs.analchem.5b04315, 2016.
- Demou, E., Visram, H., Donaldson, D. J. and Makar, P. A.: Uptake of water by organic films: The dependence on the film oxidation state, *Atmos. Environ.*, 37(25), 3529–3537, doi:10.1016/S1352-2310(03)00430-8, 2003.
- Gallimore, P. J., Griffiths, P. T., Pope, F. D., Reid, J. P. and Kalberer, M.: Comprehensive modeling study of ozonolysis of oleic acid aerosol based on real-time, online measurements of aerosol composition, *J. Geophys. Res.*, 122(8), 4364–4377, doi:10.1002/2016JD026221, 2017.
- Hosny, N. A., Fitzgerald, C., Vyšniauskas, A., Athanasiadis, A., Berkemeier, T., Uygur, N., Pöschl, U., Shiraiwa, M., Kalberer, M., Pope, F. D. and Kuimova, M. K.: Direct imaging of changes in aerosol particle viscosity upon hydration and chemical aging, *Chem. Sci.*, 7(2), 1357–1367, doi:10.1039/c5sc02959g, 2016.
- 245 Huang, D. D., Zhu, S., An, J., Wang, Q., Qiao, L., Zhou, M., He, X., Ma, Y., Sun, Y., Huang, C., Yu, J. Z. and Zhang, Q.: Comparative Assessment of Cooking Emission Contributions to Urban Organic Aerosol Using Online Molecular Tracers and Aerosol Mass Spectrometry Measurements, *Environ. Sci. Technol.*, 55(21), 14526–14535, doi:10.1021/acs.est.1c03280, 2021.
- Hung, H. and Tang, C.: Effects of Temperature and Physical State on Heterogeneous Oxidation of Oleic Acid Droplets with Ozone, *J. Phys. Chem. A*, 114(50), 13104–13112, doi:10.1021/jp105042w, 2010.
- 255 Katrib, Y., Martin, S. T., Rudich, Y., Davidovits, P., Jayne, J. T. and Worsnop, D. R.: Density changes of aerosol particles as a result of chemical reaction, *Atmos. Chem. Phys.*, 5(1), 275–291, doi:10.5194/acp-5-275-2005, 2005.
- King, M. D., Thompson, K. C. and Ward, A. D.: Laser tweezers raman study of optically trapped aerosol droplets of seawater and oleic acid reacting with ozone: Implications for cloud-droplet properties, *J. Am. Chem. Soc.*, 126(51), 16710–16711, doi:10.1021/ja044717o, 2004.
- 260 King, M. D., Rennie, A. R., Thompson, K. C., Fisher, F. N., Dong, C. C., Thomas, R. K., Pfrang, C. and Hughes, A. V.: Oxidation of oleic acid at the air-water interface and its potential effects on cloud critical supersaturations, *Phys. Chem. Chem. Phys.*, 11(35), 7699–7707, doi:10.1039/b906517b, 2009.
- King, M. D., Jones, S. H., Lucas, C. O. M., Thompson, K. C., Rennie, A. R., Ward, A. D., Marks, A. A., Fisher, F. N., Pfrang, C., Hughes, A. V. and Campbell, R. A.: The reaction of oleic acid monolayers with gas-phase ozone at the air water interface: The effect of sub-phase viscosity, and inert secondary components, *Phys. Chem. Chem. Phys.*, 22(48), 28032–28044, doi:10.1039/d0cp03934a, 2020.
- 265 Kirpes, R. M., Bonanno, D., May, N. W., Fraund, M., Barget, A. J., Moffet, R. C., Ault, A. P. and Pratt, K. A.: Wintertime Arctic Sea Spray Aerosol Composition Controlled by Sea Ice Lead Microbiology, *ACS Cent. Sci.*, 5(11), 1760–1767, doi:10.1021/acscentsci.9b00541, 2019.
- 270 Klepeis, N. E., Nelson, W. C., Ott, W. R., Robinson, J. P., Tsang, A. M., Switzer, P., Behar, J. V., Hern, S. C. and Engelmann, W. H.: The National Human Activity Pattern Survey (NHAPS): A resource for assessing exposure to environmental pollutants, *J. Expo. Anal. Environ. Epidemiol.*, 11(3), 231–252, doi:10.1038/sj.jea.7500165, 2001.
- Koop, T., Bookhold, J., Shiraiwa, M. and Pöschl, U.: Glass transition and phase state of organic compounds: Dependency on molecular properties and implications for secondary organic aerosols in the atmosphere, *Phys. Chem. Chem. Phys.*, 13(43),



- 275 19238–19255, doi:10.1039/c1cp22617g, 2011.
- Liu, Y., Bé, A. G., Or, V. W., Alves, M. R., Grassian, V. H. and Geiger, F. M.: Challenges and Opportunities in Molecular-Level Indoor Surface Chemistry and Physics, *Cell Reports Phys. Sci.*, 1(11), 100256, doi:10.1016/j.xcrp.2020.100256, 2020.
- Liu, Y., Misztal, P. K., Arata, C., Weschler, C. J., Nazaroff, W. W. and Goldstein, A. H.: Observing ozone chemistry in an occupied residence, *Proc. Natl. Acad. Sci. U. S. A.*, 118(6), doi:10.1073/pnas.2018140118, 2021.
- 280 Milsom, A., Squires, A. M., Boswell, J. A., Terrill, N. J., Ward, A. D. and Pfrang, C.: An organic crystalline state in ageing atmospheric aerosol proxies: Spatially resolved structural changes in levitated fatty acid particles, *Atmos. Chem. Phys.*, 21(19), 15003–15021, doi:10.5194/acp-21-15003-2021, 2021a.
- Milsom, A., Squires, A. M., Woden, B., Terrill, N. J., Ward, A. D. and Pfrang, C.: The persistence of a proxy for cooking emissions in megacities: a kinetic study of the ozonolysis of self-assembled films by simultaneous small and wide angle X-ray scattering (SAXS/WAXS) and Raman microscopy, *Faraday Discuss.*, 226, 364–381, doi:10.1039/D0FD00088D, 2021b.
- 285 Milsom, A., Squires, A. M., Quant, I., Terrill, N. J., Huband, S., Woden, B., Cabrera-Martinez, E. R. and Pfrang, C.: Exploring the Nanostructures Accessible to an Organic Surfactant Atmospheric Aerosol Proxy, *J. Phys. Chem. A*, doi:10.1021/acs.jpca.2c04611, 2022a.
- Milsom, A., Lees, A., Squires, A. M. and Pfrang, C.: MultilayerPy (v1.0): a Python-based framework for building, running and optimising kinetic multi-layer models of aerosols and films, *Geosci. Model Dev.*, 15(18), 7139–7151, doi:10.5194/gmd-15-7139-2022, 2022b.
- 290 Milsom, A., Squires, A. M., Ward, A. D. and Pfrang, C.: The impact of molecular self-organisation on the atmospheric fate of a cooking aerosol proxy, *Atmos. Chem. Phys.*, 22(7), 4895–4907, doi:10.5194/acp-22-4895-2022, 2022c.
- Mu, Q., Shiraiwa, M., Octaviani, M., Ma, N., Ding, A., Su, H., Lammel, G., Pöschl, U. and Cheng, Y.: Temperature effect on phase state and reactivity controls atmospheric multiphase chemistry and transport of PAHs, *Sci. Adv.*, 4(3), eaap7314, doi:10.1126/sciadv.aap7314, 2018.
- 295 Müller, M., Mishra, A., Berkemeier, T., Hausammann, E., Peter, T. and Krieger, U. K.: Electrodynamic balance–mass spectrometry reveals impact of oxidant concentration on product composition in the ozonolysis of oleic acid, *Phys. Chem. Chem. Phys.*, doi:10.1039/D2CP03289A, 2022.
- 300 Or, V. W., Alves, M. R., Wade, M., Schwab, S., Corsi, R. L. and Grassian, V. H.: Crystal Clear? Microspectroscopic Imaging and Physicochemical Characterization of Indoor Depositions on Window Glass, *Environ. Sci. Technol. Lett.*, 5(8), 514–519, doi:10.1021/acs.estlett.8b00355, 2018.
- Or, V. W., Wade, M., Patel, S., Alves, M. R., Kim, D., Schwab, S., Przelomski, H., O'Brien, R., Rim, D., Corsi, R. L., Vance, M. E., Farmer, D. K. and Grassian, V. H.: Glass surface evolution following gas adsorption and particle deposition from indoor cooking events as probed by microspectroscopic analysis, *Environ. Sci. Process. Impacts*, 22(8), 1698–1709, doi:10.1039/d0em00156b, 2020.
- 305 Osterroht, C.: Extraction of dissolved fatty acids from sea water, *Fresenius. J. Anal. Chem.*, 345(12), 773–779, doi:10.1007/BF00323009, 1993.



- Ots, R., Vieno, M., Allan, J. D., Reis, S., Nemitz, E., Young, D. E., Coe, H., Di Marco, C., Detournay, A., Mackenzie, I. A.,
310 Green, D. C. and Heal, M. R.: Model simulations of cooking organic aerosol (COA) over the UK using estimates of emissions
based on measurements at two sites in London, *Atmos. Chem. Phys.*, 16(21), 13773–13789, doi:10.5194/acp-16-13773-2016,
2016.
- Ovadnevaite, J., Zuend, A., Laaksonen, A., Sanchez, K. J., Roberts, G., Ceburnis, D., Decesari, S., Rinaldi, M., Hodas, N.,
Facchini, M. C., Seinfeld, J. H. and O'Dowd, C.: Surface tension prevails over solute effect in organic-influenced cloud droplet
315 activation, *Nature*, 546(7660), 637–641, doi:10.1038/nature22806, 2017.
- Patel, S., Sankhyan, S., Boedicker, E. K., Decarlo, P. F., Farmer, D. K., Goldstein, A. H., Katz, E. F., Nazaroff, W. W., Tian,
Y., Vanhanen, J. and Vance, M. E.: Indoor Particulate Matter during HOMEChem: Concentrations, Size Distributions, and
Exposures, *Environ. Sci. Technol.*, 54(12), 7107–7116, doi:10.1021/acs.est.0c00740, 2020.
- Pfrang, C., Shiraiwa, M. and Pöschl, U.: Chemical ageing and transformation of diffusivity in semi-solid multi-component
320 organic aerosol particles, *Atmos. Chem. Phys.*, 11(14), 7343–7354, doi:10.5194/acp-11-7343-2011, 2011.
- Pfrang, C., Rastogi, K., Cabrera-Martinez, E. R., Seddon, A. M., Dicko, C., Labrador, A., Plivelic, T. S., Cowieson, N. and
Squires, A. M.: Complex three-dimensional self-assembly in proxies for atmospheric aerosols, *Nat. Commun.*, 8(1), 1724,
doi:10.1038/s41467-017-01918-1, 2017.
- Pöschl, U., Rudich, Y. and Ammann, M.: Kinetic model framework for aerosol and cloud surface chemistry and gas-particle
325 interactions - Part 1: General equations, parameters, and terminology, *Atmos. Chem. Phys.*, 7(23), 5989–6023,
doi:10.5194/acp-7-5989-2007, 2007.
- Reynolds, J. C., Last, D. J., McGillen, M., Nijs, A., Horn, A. B., Percival, C., Carpenter, L. J. and Lewis, A. C.: Structural
analysis of oligomeric molecules formed from the reaction products of oleic acid ozonolysis, *Environ. Sci. Technol.*, 40(21),
6674–6681, doi:10.1021/es060942p, 2006.
- 330 Robinson, A. L., Donahue, N. M. and Rogge, W. F.: Photochemical oxidation and changes in molecular composition of organic
aerosol in the regional context, *J. Geophys. Res.*, 111(D3), D03302, doi:10.1029/2005JD006265, 2006.
- Rudich, Y.: Laboratory Perspectives on the Chemical Transformations of Organic Matter in Atmospheric Particles, *Chem.
Rev.*, 103(12), 5097–5124, doi:10.1021/cr020508f, 2003.
- Schwartz-Narbonne, H. and Donaldson, D. J.: Water uptake by indoor surface films, *Sci. Rep.*, 9(1), 11089,
335 doi:10.1038/s41598-019-47590-x, 2019.
- Sebastiani, F., Campbell, R. A. and Pfrang, C.: Night-time oxidation at the air-water interface: co-surfactant effects in binary
mixtures, *Environ. Sci. Atmos.*, 1324–1337, doi:10.1039/d2ea00056c, 2022.
- Shiraiwa, M., Pfrang, C. and Pöschl, U.: Kinetic multi-layer model of aerosol surface and bulk chemistry (KM-SUB): The
influence of interfacial transport and bulk diffusion on the oxidation of oleic acid by ozone, *Atmos. Chem. Phys.*, 10, 3673–
340 3691, doi:10.5194/acp-10-3673-2010, 2010.
- Shiraiwa, M., Ammann, M., Koop, T. and Pöschl, U.: Gas uptake and chemical aging of semisolid organic aerosol particles,
Proc. Natl. Acad. Sci. U. S. A., 108(27), 11003–11008, doi:10.1073/pnas.1103045108, 2011.



- Shiraiwa, M., Pfrang, C., Koop, T. and Pöschl, U.: Kinetic multi-layer model of gas-particle interactions in aerosols and clouds (KM-GAP): Linking condensation, evaporation and chemical reactions of organics, oxidants and water, *Atmos. Chem. Phys.*, 12(5), 2777–2794, doi:10.5194/acp-12-2777-2012, 2012.
- Shrivastava, M., Lou, S., Zelenyuk, A., Easter, R. C., Corley, R. A., Thrall, B. D., Rasch, P. J., Fast, J. D., Simonich, S. L. M., Shen, H. and Tao, S.: Global long-range transport and lung cancer risk from polycyclic aromatic hydrocarbons shielded by coatings of organic aerosol, *Proc. Natl. Acad. Sci. U. S. A.*, 114(6), 1246–1251, doi:10.1073/pnas.1618475114, 2017.
- Voinova, M. V, Rodahl, M., Jonson, M. and Kasemo, B.: Viscoelastic Acoustic Response of Layered Polymer Films at Fluid-Solid Interfaces: Continuum Mechanics Approach, *Phys. Scr.*, 59(5), 391–396, doi:10.1238/physica.regular.059a00391, 1999.
- Wang, Q. and Yu, J. Z.: Ambient Measurements of Heterogeneous Ozone Oxidation Rates of Oleic, Elaidic, and Linoleic Acid Using a Relative Rate Constant Approach in an Urban Environment, *Geophys. Res. Lett.*, 48(19), doi:10.1029/2021GL095130, 2021.
- Wang, Q., He, X., Zhou, M., Huang, D. D., Qiao, L., Zhu, S., Ma, Y. G., Wang, H. L., Li, L., Huang, C., Huang, X. H. H., Xu, W., Worsnop, D., Goldstein, A. H., Guo, H., Yu, J. Z., Huang, C. and Yu, J. Z.: Hourly Measurements of Organic Molecular Markers in Urban Shanghai, China: Primary Organic Aerosol Source Identification and Observation of Cooking Aerosol Aging, *ACS Earth Sp. Chem.*, 4(9), 1670–1685, doi:10.1021/acsearthspacechem.0c00205, 2020.
- Woden, B., Skoda, M., Milsom, A., Maestro, A., Tellam, J. and Pfrang, C.: Ozonolysis of fatty acid monolayers at the air-water interface: organic films may persist at the surface of atmospheric aerosols, *Atmos. Chem. Phys. Discuss.*, 1–26, doi:10.5194/acp-2020-717, 2020.
- Zahardis, J. and Petrucci, G. A.: The oleic acid-ozone heterogeneous reaction system: products, kinetics, secondary chemistry, and atmospheric implications of a model system-a review. [online] Available from: www.atmos-chem-phys.net/7/1237/2007/, 2007.
- Zahardis, J., LaFranchi, B. W. and Petrucci, G. A.: Direct observation of polymerization in the oleic acid-ozone heterogeneous reaction system by photoelectron resonance capture ionization aerosol mass spectrometry, *Atmos. Environ.*, 40(9), 1661–1670, doi:10.1016/j.atmosenv.2005.10.065, 2006a.
- Zahardis, J., LaFranchi, B. W. and Petrucci, G. A.: Photoelectron resonance capture ionization mass spectrometry of fatty acids in olive oil, *Eur. J. Lipid Sci. Technol.*, 108(11), 925–935, doi:10.1002/ejlt.200600143, 2006b.